

# Preparation and Characterization of PMMA–Clay Hybrid Composite by Emulsion Polymerization

DONG CHOO LEE and LEE WOOK JANG

Department of Polymer Science and Engineering, Inha University, Incheon, 402-751, South Korea

## SYNOPSIS

Nanocomposites are prepared by a simple technique of emulsion polymerization using MMA monomer and Na<sup>+</sup>-montmorillonite. The products are purified by hot toluene extraction and characterized by FT-IR, X-ray diffraction, TGA, DSC, and tensile testing. The structural investigation confirms that the products are intercalated with PMMA chain molecules oriented parallel to the direction of lamellar layers whose separation is consequently more enlarged than in the polymer-free clay. DSC traces also corroborate the confinement of the polymer in the inorganic layer by exhibiting no observable transition in the thermogram. Both the thermal stability and tensile properties of the products appear to be substantially enhanced. The ion–dipole bonding is believed to be the driving force for the introduction and fixation of the organic polymer to the interfaces of montmorillonite.

© 1996 John Wiley & Sons, Inc.

## INTRODUCTION

In recent years, the high tech uses of clays are expanding. This is due, in great part, to the recent developments of new functionalization of smectic clays whereby a large number of polymer–clay nanocomposites become accessible in the form of end-functionalized derivatives.<sup>1–5</sup> This type of organic–inorganic nanocomposites can potentially show hybrid properties synergistically derived from both the host (clay) and the guest (polymer).<sup>6</sup>

The structural characteristics of montmorillonite, a smectic clay, are the octahedral aluminate sheet sandwiched between tetrahedral silicate layers, and the layer charge can easily be generated by replacement of cations in the layer with cations of different charges; e.g., replacement of Al<sup>3+</sup> in the aluminate sheet with Mg<sup>2+</sup> or Fe<sup>2+</sup> produces negatively charged aluminate layers, and cations (Na<sup>+</sup> or K<sup>+</sup>) are newly incorporated into the interlayer spaces to maintain charge neutrality.<sup>7</sup> Hence, in the case where the interlayer is incorporated with Na<sup>+</sup>, the hydrophilic property must be enhanced, which in turn leads to easy penetration and high degree of water swelling.

Thus, it is anticipated that this structural characteristics of the montmorillonite can possibly provide an effective method for the preparation of a hybrid composite intercalated with polymer in the layered host if an aqueous system is involved in the intercalation procedure.

Accordingly, in the present investigation, a new procedure using an emulsion system for the intercalation of Na<sup>+</sup> exchanged montmorillonite with PMMA has been attempted. An emulsion polymerization in which an MMA monomer is dispersed in a water phase and polymerized with a water soluble radical initiator has been carried out in the presence of Na<sup>+</sup> exchanged montmorillonite. The present paper discusses on the results obtained from the structural study and material characterization of nanocomposites prepared by above-mentioned emulsion polymerization.

## EXPERIMENTAL

### Materials

Bentonite provided by the Tae-Kwang Chem. Co. has a 70% montmorillonite content and 90 mEq/100 g of ion exchange capacity. The clay was purified by dispersion of this crude clay into distilled water

and separation of the noncolloidal impurities. To obtain cation exchange, the purified clay was suspended in an aqueous solution of  $\text{Na}_2\text{CO}_3$  for 24 h with agitation at  $40^\circ\text{C}$ , repeatedly washed with distilled water, and separated by centrifugation. The product, dried under reduced pressure at  $70^\circ\text{C}$ , was ball-milled and sieved to 325 mesh.

### Emulsion Polymerization

A heterogeneous reaction in which a distilled MMA monomer is dispersed in a continuous water phase with the aid of sodium lauryl sulfate and polymerized with potassium persulfate in the presence of  $\text{Na}^+$ -montmorillonite was carried out at  $70^\circ\text{C}$  for 12 h. Being coagulated by the addition of aluminum sulfate solution, the product was filtered and dried under reduced pressure.

### Characterization and Measurements

A part of the pulverized product was extracted with hot toluene for five days by means of the Soxhlet extraction. The content of intercalated polymer was determined by thermogravimetric analysis (TGA) for those extracted or nonextracted samples. The polymers recovered from the extracts are subjected to GPC measurements to obtain the average molecular mass and its polydispersity. A Waters Model 201 equipped with a U6K injector, a M 6000A solvent delivery system, a M 730 data module, and three linear columns packed with  $\mu$ -Styragel were used. The flow rate of THF was 1.0 mL/min. The Fourier transform infrared (FT-IR) spectra for all the composites extracted and the polymers recovered from the extracts were recorded on a Nicolet spectrophotometer in the range of  $4000\text{--}400\text{ cm}^{-1}$ . The KBr pellet method was used. The thermal properties of the composites were measured by differential scanning calorimetry (DSC). A DuPont 2100 was used. Samples of 10-mg masses were heated in nitrogen atmosphere to  $300^\circ\text{C}$  at a heating rate  $10^\circ\text{C}/\text{min}$ . Being cooled to room temperature, heating was repeated with the same heating rate. The data obtained from the second scanning were accepted. TGA measurements were carried out by employing a DuPont 9900 thermogravimetric analyzer. Samples of 20 mg masses were heated to  $500^\circ\text{C}$  at a heating rate of  $20^\circ\text{C}/\text{min}$  under nitrogen atmosphere. X-ray diffraction (XRD) patterns were recorded by monitoring the diffraction angle  $2\theta$  from 2 to 32 degrees on a Philip PW-1847 X-ray crystallographic unit mounted with a Guinier focusing camera. The unit was equipped with Ni-filtered  $\text{CuK } \alpha$  radiation

source operated at 40 KV and 20 mA. The scanning speed, the step size, and the time per step were  $0.016\ 2\theta/\text{sec}$ ,  $0.02^\circ$ , and 1.25 sec, respectively. Silicon crystal was used as a calibration standard. The stress-strain behavior of the composite was observed by the tensile testing. An Instron (Instron Co. Series IX Automated Materials Testing System 1.16) operated with a chart speed of 5 pts/sec, and a cross-head speed of 1.27 mm/min was used. The dumbbell specimens were molded on the Mini-Max Injection Molder (Model CS-183, Custom Scientific Instruments, Inc.) set at  $220 \pm 5^\circ\text{C}$ . The mass needed to mold a specimen was approximately 0.3 g. The tests were carried out at  $25^\circ\text{C}$  and 60% relative humidity.

## RESULTS AND DISCUSSION

### Structural Characterization

A composite intercalated with PMMA was simply obtained by an emulsion polymerization of MMA in the presence of  $\text{Na}^+$ -montmorillonite, without employing any modification of monomer to impart active site or without the addition of any coupling agents. The products thus obtained were exposed to boiling toluene for five days to remove those non-bonded organic materials. As are exhibited in Table I, products holding unextractable organic materials, which can be regarded as the bonded PMMA, reveal different quantities of bound polymer, according to what the input ratios of monomer and montmorillonite were. The trend appears to be that the contents of polymer unextractable are inversely proportional to the amounts of montmorillonite added.

Figure 1 shows a representative diagram illustrating the variations of polymer content against

**Table I** The Input Ratio and The Contents of PMMA in the Composites

Sample Code	Input Ratio of MMA/MMT <sup>a</sup> (g/g)	PMMA Content in Product (wt %)	
		A <sup>b</sup>	B <sup>c</sup>
JMM10	100/10	87.4	58.7
JMM20	100/20	79.3	49.6
JMM30	100/30	60.4	33.4
JMM40	100/40	58.6	22.8
JMM50	100/50	46.1	18.4

<sup>a</sup> Montmorillonite.

<sup>b</sup> A, products not purified by extraction.

<sup>c</sup> B, products purified by hot toluene extraction for 5 days.

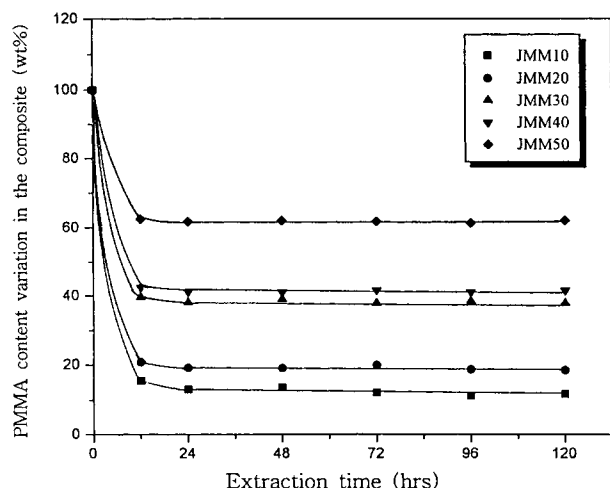


**Figure 1** PMMA content variations of composites as a function of extraction times.

extraction hours. Evidently, a considerable amount of the unextractable polymer still remained, even after 120 h of extraction. The residual PMMA is regarded as the polymer intercalated between the interlayers of clay. This confinement of the polymer in the interlayer of clay is tentatively ascribed to both the ion-dipole force acting between the host (clay) and the guest (PMMA) and the contraction of the gallery height due to the water removal from the gallery. Figure 1 also demonstrates that the most of the nonbonded organic materials can be eliminated from the composite by 24 h of extraction.

Table II shows the average molecular masses and polydispersities of PMMA obtained from the polymerization with exclusion of clay and those obtained by precipitation with nonsolvent addition to the extracts of the composites. All those  $M_w$  values exhibited by the polymer obtained from the composite extracts are in the order of  $10^5$  g/mol and are comparable with that of pure PMMA polymerization, suggesting that the presence of clay does not significantly affect the average molecular mass of the polymer intercalated. Hence, it seems plausible that the average molecular masses of polymer being intercalated, though not decisive, may be equivalent to those listed in Table II.

Evidence of polymer intercalation is obtained from the analysis of IR spectrum recorded for the extracted composites. Figure 2 illustrates those spectra obtained from the pure PMMA, Na<sup>+</sup>-montmorillonite, and extracted composite materials. From the spectra recorded for the extracted composites, the presence of both the characteristic group frequencies of PMMA and montmorillonite can be found. The absorption bands at 3630, 1050, and

those between 600–400  $\text{cm}^{-1}$  can be associated respectively with —OH stretching of the lattice water, Si–O stretching, and Al–O stretching, and Si–O bending. Concurrently, those bands at 3000–2900  $\text{cm}^{-1}$  (—CH<sub>3</sub> stretching), 1735  $\text{cm}^{-1}$  (C=O stretching), and 1300–1100  $\text{cm}^{-1}$  (C–O stretching) are the consequence due to the characteristic frequencies of PMMA. Moreover, the fact that no evidence of new absorption bands can be found in the spectrum suggests there are no primary valence forces involved between host and guest, indicating that the confinement of polymers in the host's layer occurs mainly by the secondary valence force.

Further evidence for the intercalation can be obtained from the XRD patterns of the purified composite. As shown by the powder patterns in Figure 3, all the composites contain those diffraction peaks characteristic of the pristine Na<sup>+</sup>-montmorillonite, which suggests the composite remains crystalline over the range of PMMA content studied. Most prominently, however, the 001  $d$ -spacings of the composites were found to be changed in height. Hence, the variations of  $d_{001}$  value are calculated and summarized in Table III. Evidently, the  $d$ -spacings are increased with the increments of PMMA content in the composites more than that of pristine montmorillonite. It is this phenomenon that makes it clear that the composites are intercalated with the guest polymer. Except for the cases in which the higher ratios of montmorillonite are concerned, the average interlayer distances of composites are enlarged as much as 0.54 nm, which is comparable with 0.68 nm obtained from the intercalation of alkylammonium montmorillonite with PS,<sup>4</sup> but is slightly lower than 0.83 nm, resulting from the functionalization of montmorillonite by PMMA containing side-chain ammonium cations.<sup>3</sup> It is, therefore, worth noting that a simple emulsion polymerization can also lead to the production of an effective nanocomposite without using any kinds of coupling

**Table II** Average Molecular Masses and Polydispersities of PMMA Obtained From the Composite Extracts

Sample Code	$\bar{M}_n \times 10^{-4}$ (g/mol)	$\bar{M}_w \times 10^{-4}$ (g/mol)	$\bar{M}_w/\bar{M}_n$
PMMA	2.3	16.0	6.6
JMM10	4.4	25.0	5.8
JMM20	6.0	20.0	3.4
JMM30	6.3	15.0	2.4
JMM40	8.2	39.0	4.8
JMM50	3.8	29.0	7.6

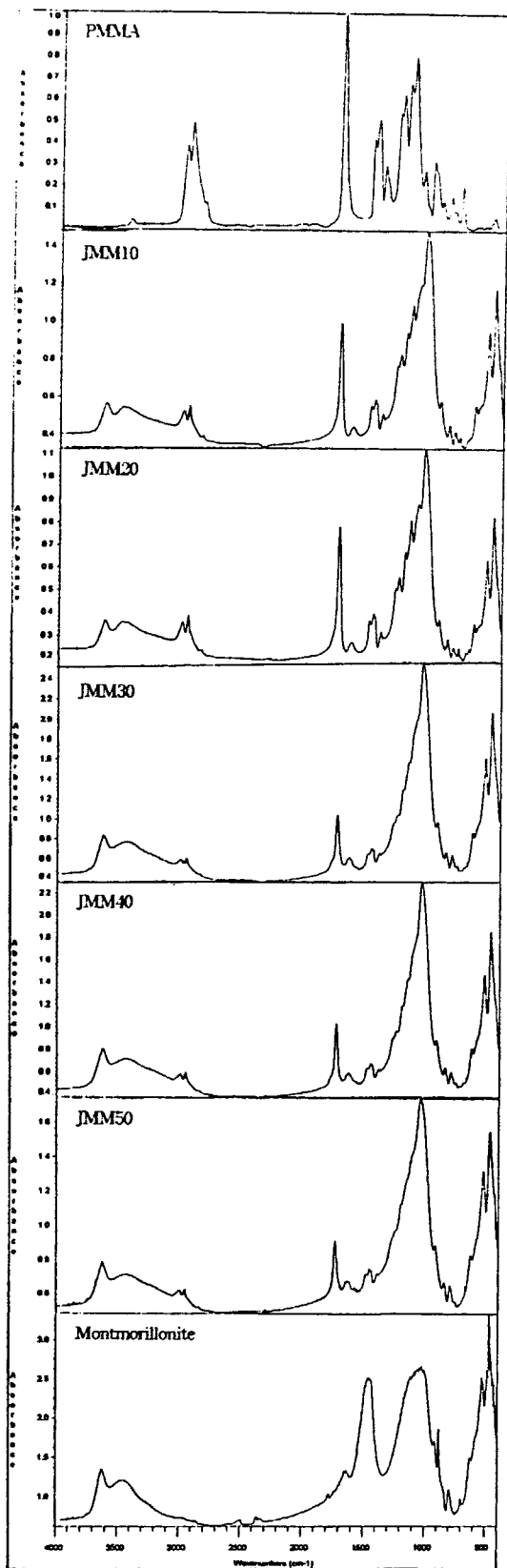


Figure 2 IR spectra of PMMA, montmorillonite, and purified composite products.

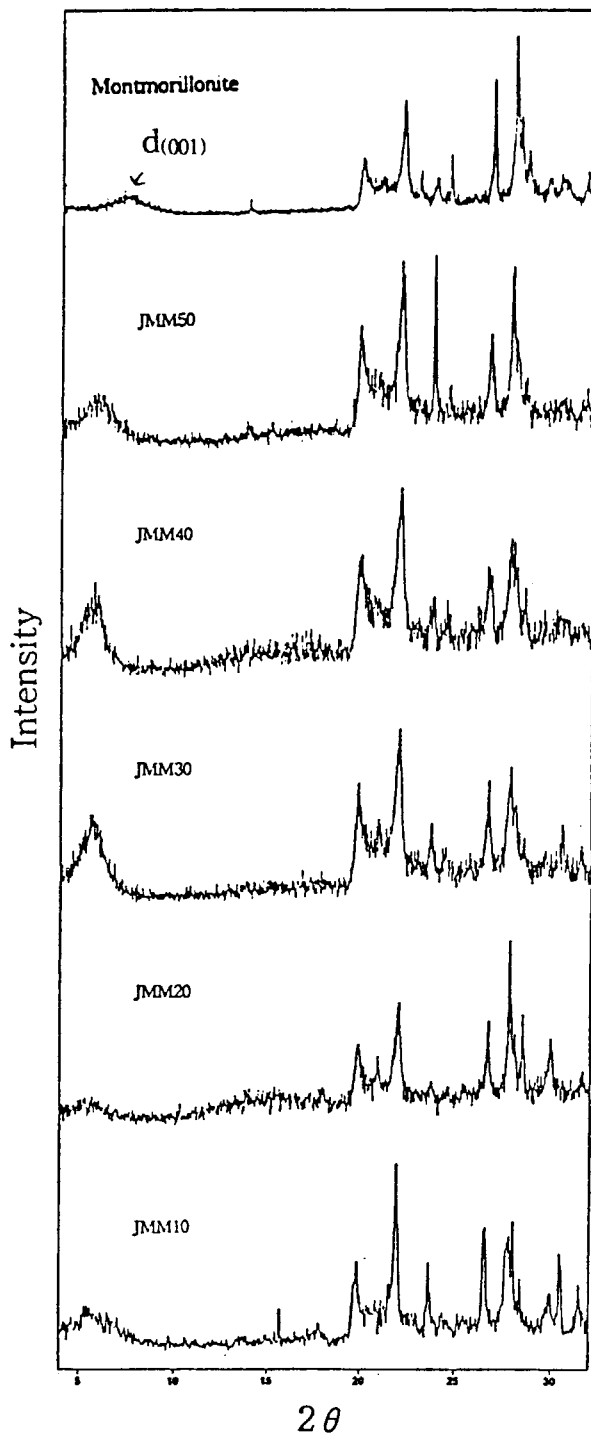


Figure 3 XRD patterns of purified composites.

agents or modifications of guest monomer or polymer to be intercalated.

In terms of this gallery expansion, additional information can be obtained for the conformational state of the intercalated polymer. The 0.54 nm of gallery increase is found to be far less than 28.6 nm

**Table III XRD Data of Composites**

Sample Code	PMMA Content (wt %)		Interlayer Distance	
	A <sup>a</sup>	B <sup>b</sup>	<i>d</i> (nm)	$\Delta$ (nm) <sup>c</sup>
MMT <sup>d</sup>	—	—	1.15	0
JMM10	87.4	58.7	1.73	0.58
JMM20	79.3	49.6	1.68	0.53
JMM30	60.4	33.4	1.67	0.52
JMM40	58.6	22.8	1.50	0.35
JMM50	46.1	18.4	1.28	0.13

<sup>a</sup> A, products not purified by extraction.

<sup>b</sup> B, products purified by hot toluene extraction for 5 days.

<sup>c</sup> Variation of interlayer distance of the montmorillonite induced by organic loading.

<sup>d</sup> Montmorillonite.

of the root-mean square end-to-end distance estimated for an unperturbed random coil of PMMA having molecular mass  $2.0 \times 10^5$  g/mol. Furthermore, the thickness measured for the MMA monomer by using a chemical model was found to be 0.64 nm, which corresponds roughly to the gallery increase. These observations lead to a conclusion that the chain molecules intercalated may assume a planar conformation oriented parallel to the direction of interlayer but with restricted segmental motion. Although enough information, on the other hand, is not available at present for the determination of interlayer numbers per unit mass of montmorillonite, a separate experimental result that the montmorillonite has shown five times the amount of swelling expansion under water can be used for a qualitative estimation that the chain molecules confined in a gallery may possibly be composed with multilayers of nearly collapsed planar chains, especially for the case of high PMMA content.

### Material Characterization

Figure 4 shows a TGA thermogram of weight loss as a function of temperature for PMMA 1 and the extracted composites. Evidently, the onset of the thermal decomposition of those composites shifted significantly toward the higher temperature range than that of PMMA, which confirms the enhancement of thermal stability of intercalated PMMA. It is also noteworthy that all those five composites exhibited nearly the same onset temperature of decomposition (340°C), regardless of their polymer contents, indicating that the thermal insulation effect of montmorillonite does not depend much on

the contents of intercalated polymer. Furthermore, all hybrid composites were found to be stable up to 340°C.

DSC traces of the pure PMMA and composites are shown in Figure 5. The pure polymer exhibits an endotherm at approximately at 102°C, corresponding to the  $T_g^8$  of PMMA. Nevertheless, the intercalated polymer does not show any traces of clear transitions. This is tentatively ascribed to the confinement of the intercalated polymer chains within the silicate galleries that prevents the segmental motions of the polymer chains.

Tensile data are summarized in Table IV. Owing to their powdery texture, the composites containing less than 70 wt % of PMMA were not suitable for mechanical measurements. The tensile modulus of the composite apparently increased in proportion to the amounts of montmorillonite. This enhancement of modulus is reasonably attributed to the high resistance exerted by the montmorillonite against the plastic deformation, together with the effect of stretching resistance of the oriented backbone bonds of polymer chain in the gallery.

The stress at maximum load also appeared to be slightly higher than that of pure PMMA. This enhancement of ultimate strength is considered to be largely responsible for the increase of toughness, being caused by the diminution of stress concentration at the crack tip due to the ligaments of intercalated polymer chains spanning a crack; hence, the fracture involves some energy dissipation.<sup>9</sup>

### CONCLUSION

The most striking results obtained from the above experiments are the demonstrations of direct inter-

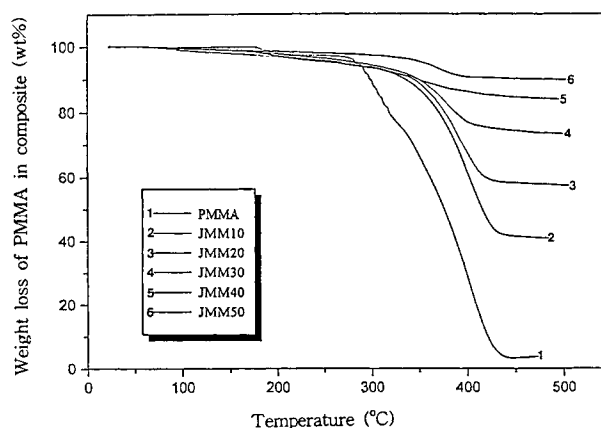


**Figure 4** TGA thermogram of weight loss as a function of temperature for pure PMMA (1) and purified composites (2–6).

calation in the smectite type of clay by a simple emulsion polymerization and the enhanced properties of the intercalated products. The structural analysis of the composite confirms that the PMMA chains are confined between the interlayer of montmorillonite in the form of stretched planar type of conformation. In contrast to the bulk PMMA, the intercalated polymer does not show any clear DSC endotherm, which suggests the segmental motions of the polymer chains within the interlayer of montmorillonite are highly restricted.

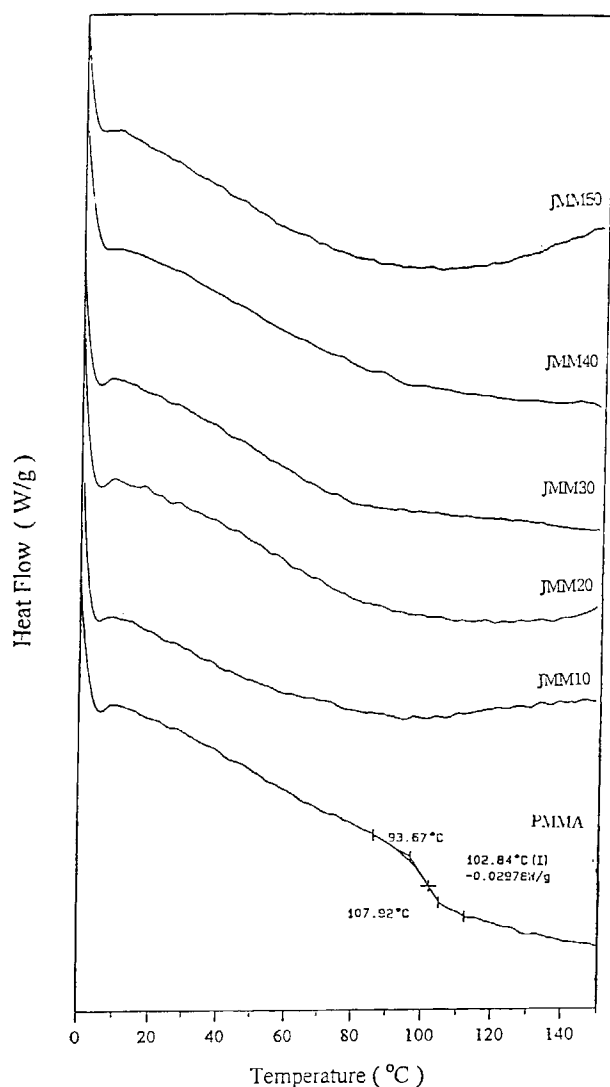


**Figure 5** DSC thermogram of pure PMMA and composites.

**Table IV** Instron Data of Composites and Pure PMMA

Sample Code	Stress at Max. Load (MPa)	Strain at Max. Load (%)	Young's Modulus (GPa)
PMMA	53.95	4.23	3.06
JMM10	62.02	4.25	4.64
JMM20	62.03	2.84	4.89

The enhanced thermal stability of the composite was also corroborated by the TGA experiment. The onset temperature of decomposition found was about 340°C, regardless of the polymer contents in the composite. The composite containing 10 wt % montmorillonite yielded tensile strength and modulus values, respectively, of 62.0 MPa and 4.64 GPa. These were higher increases than the values resulting from the pristine polymer of 53.9 MPa and 3.06 GPa.

The strong fixation of polymer to the inorganic surfaces is considered to be due to the cooperative formation of ion-dipole forces.

The authors gratefully acknowledge supporting grants from the Division of Research of Inha University.

## REFERENCES

1. L. Tie, P. D. Kaviratna, and T. J. Pinnavaia, *Chem. Mater.*, **6**, 573 (1994).
2. M. S. Wang and T. J. Pinnavaia, *Chem. Mater.*, **6**, 464 (1994).
3. L. Biasci, M. Aglietto, G. Ruggeri, and F. Ciardelli, *Polymer*, **35**, 3296 (1994).
4. R. A. Vaia, H. Ishii, and E. P. Giannelis, *Chem. Mater.*, **5**, 1694 (1993).
5. U. Usuki, Y. Fukushima, M. Fujimoto, Y. Kojima, and O. Kamigaito, U.S. Pat. 4,889,885 (1989).
6. L. F. Nazar, Z. Zhang, and D. Zinkweg, *J. Am. Chem. Soc.*, **114**, 6239 (1992).
7. A. Weiss, *Angew. Chem. Int. Ed. Engl.*, **2**, 134 (1963).
8. J. Brandrup and E. H. Immergut, *Polymer Handbook*, 3rd ed., Wiley-Interscience, pp. VI-219.
9. A. J. Kinloch and R. J. Young, *Fracture Behavior of Polymers*, Elsevier, 1985, p. 423.

Received December 5, 1995

Accepted January 28, 1996